

Origin of the Optical Gap in Half-Doped Manganites

Mario Cuoco,¹ Canio Noce,¹ and Andrzej M. Oles^{2,3}

¹*I.N.F.M. -Unità di Salerno, Dipartimento di Fisica "E.R. Caianiello",
Università di Salerno, Via S. Allende, I-84081 Baronissi, Italy*

²*Marian Smoluchowski Institute of Physics, Jagellonian University, Reymonta 4, PL-30059 Kraków, Poland*

³*Max-Planck-Institut für Festkörperforschung, Heisenbergstrasse 1, D-70569 Stuttgart, Germany*

We have analyzed the coexisting charge and orbital ordering in half-doped manganites using a model which includes Coulomb and Jahn-Teller orbital polarization interactions. Most surprisingly, the gap in the optical conductivity is reduced by both on-site and intersite Coulomb interactions, but increases and explains the experimental results when the Jahn-Teller terms with orbital polarization are considered. The origin of this behavior is explained within a molecular model which arises in the limit of extreme topological frustration, when single electrons are confined to molecular units consisting of three orbitals.

I. INTRODUCTION

The colossal magnetoresistance (CMR) manganites form a class of materials in which the problem of the interplay between the spin, orbital, and charge degrees of freedom is believed to lie at the heart of understanding their physical properties.^{1,2} The parent compound, LaMnO₃, is a Mott insulator due to large local Coulomb interaction U , with a single electron localized in degenerate e_g orbitals at Mn³⁺ ions. The magnetic and orbital ordering follow then from superexchange interactions which stabilize antiferromagnetic (AF) order.³ The doping by holes adds the charge degree of freedom in systems like La_{1-x}Sr_xMnO₃, and triggers a transition to ferromagnetic (FM) state, in which the kinetic energy of the doped e_g holes is optimized. This mechanism, called double exchange, was postulated five decades ago by Zener.⁴ Yet, the AF order is favored again at half doping ($x = 0.5$),^{2,6} indicating that the AF superexchange and the FM double exchange frustrate each other, as in the FM metallic phase.⁷

The half-doped manganites are very peculiar, and exhibit a so-called charge exchange (CE) AF ordering,^{5,6} which involves FM zigzag chains that are staggered antiferromagnetically; it has been observed experimentally by neutron scattering^{8,9} and by X-ray diffraction,^{10,11} both in the one-plane La_{0.5}Sr_{1.5}MnO₄,^{8,10} and in cubic Nd_{0.5}Sr_{0.5}MnO₃ manganites.^{9,11} The mechanism of stability of the CE phase is still under debate. The hopping between degenerate e_g orbitals along zigzag chains shows a *topological frustration*¹² which leads to a band insulator.^{13,14} Although the CE phase is then favored, the large on-site Coulomb element U destabilizes it for realistic parameters.¹⁵ Therefore, one expects that either intersite Coulomb interactions,^{16,17} or the coupling to the lattice which leads to the Jahn-Teller (JT) distortions,^{18,19} might play an important role.

We argue that, similar as for the FM metallic phase,²⁰ the optical experiments may provide the clue to the proper understanding of the CE phase within a truly

relevant microscopic model. The experiments for the La_{0.5}Sr_{1.5}MnO₄ compound^{21,22} show peculiar features by decreasing temperature from 300 K to 10 K. Above the charge/orbital transition $T_{CO} \simeq 217$ K, the midinfrared spectrum is broad with an optical gap of the order of 0.2 eV and a width of about 1.5 eV. It centers around the main peak at ~ 0.8 eV. Below T_{CO} one observes a rigid shift toward high energy and a narrowing of the spectrum. At the same time, the main peak shifts towards the bottom of the spectrum, giving rise to an asymmetric profile of the optical curve and an increase of the spectral weight. Finally, as the temperature is lowered below the Néel temperature $T_N \simeq 110$ K, a further slight and smooth increase of the optical gap and narrowing of the main peak are observed.

On the theoretical side, there have been only few reports on the optical properties of the charge and orbital ordering in half-doped manganites,^{22,23} based on the electronic structure calculations. In fact, these studies can serve as a starting point for the analysis of the correlated character of the optical excitations in the case of e_g electrons which are coupled either via the Coulomb interaction, or via the JT distortions.

In this paper we introduce a new microscopic model for half-doped manganites. Next to the on-site Coulomb repulsion, it includes the JT term responsible for the e_g orbital polarization at Mn³⁺ ions, induced by the JT distortions around the occupied sites when holes occupy the neighboring Mn⁴⁺ ions.^{6,24} We study this model by exact diagonalization (ED) using Lanczos algorithm,²⁵ and investigate: (i) the microscopic origin of the CE phase, its stability and properties in presence of the JT terms, (ii) the nature of the optical excitations as due to transitions between the correlated states of e_g electrons at Mn($3d^4$) sites, and (iii) the reasons for the peculiar changes observed in the optical spectra under increasing temperature.^{21,22} The unexpected result of the reduction of the charge gap due to electron correlations is explained as a consequence of the subtle role played by the topological frustration. This behavior turns out to be relevant

in explaining the pseudogap like features observed in the optical spectrum of the high temperature phase, where the distortions are weak and the charge and orbital correlations are only at short range. Furthermore, we show that the large optical gap observed in $\text{La}_{0.5}\text{Sr}_{1.5}\text{MnO}_4$ at low temperature²¹ cannot be simply explained within neither the electronic structure theory,²³ nor using a correlated band insulator,¹⁴ but instead by including the JT interaction.

The paper is organized as follows. In Sec. II we present the model Hamiltonian (Sec. II.A) and discuss the stability of the CE phase, using as stabilizing mechanism either the JT term, or the intersite Coulomb interaction (Sec. II.B). Next we elucidate the frustration present in the kinetic energy due to the orbital phase factors, and introduce a so-called *molecular model* (MM) in which this frustration is maximized (Sec. II.C). The optical spectra are determined and analyzed both for the CE phase and the MM in Sec. III.A. The optical gap is extrapolated to the thermodynamic limit using finite size scaling (Sec. III.B). Finally, we discuss the obtained optical spectra in a broader context of the existing experiments, and summarize our results in Sec. IV.

II. THE MODEL AND ITS GROUND STATE

A. Importance of the JT coupling

The model we adopt follows from the experimental evidence in manganites on the importance of the orbital degrees of freedom, the local Coulomb interactions $\propto U$, and the JT distortions $\propto E_{\text{JT}}$. The local Coulomb repulsion U reduces the probability of double occupancies of e_g orbitals, while the Hund's exchange coupling J_H between the e_g and the t_{2g} electrons is responsible for the high-spin states, realized both at Mn^{3+} and Mn^{4+} ions. This term will not be explicitly included, as we assume that the e_g and t_{2g} spins are aligned, which corresponds to the frequently considered limit of $J_H \rightarrow \infty$.

We consider (spinless) e_g electrons moving along a FM zigzag chain of the CE phase shown in Fig. 1. Along each chain two kinds of nonequivalent sites alternate: bridge ($i \in B$) and corner ($j \in C$) sites (see Fig. 1). The *polaronic* model,

$$\mathcal{H}_{\text{pol}} = H_t + H_U + H_{\text{JT}}, \quad (1)$$

consists of three terms,

$$H_t = \sum_{i \in B, j \in C} \left[(-1)^{\lambda_{ij}} t_1(\phi) b_i^\dagger a_{jx} - t_2(\phi) b_i^\dagger a_{jz} + \text{H.c.} \right], \quad (2)$$

$$H_U = U \sum_{j \in C} n_{jx} n_{jz}, \quad (3)$$

$$H_{\text{JT}} = \sum_i \left[g \sum_{j(i)} q_i (n_{i\zeta} - n_{i\xi}) (1 - n_j) + \frac{1}{2} k_{\text{JT}} q_i^2 \right], \quad (4)$$

which stand for the kinetic energy (H_t), the on-site (interorbital) Coulomb interaction U at corner sites (H_U), and the JT polaronic interaction (H_{JT}), respectively. The kinetic energy H_t describes the hopping $\propto t$ of e_g electrons between the directional $3x^2 - r^2$ ($3y^2 - r^2$) orbitals at bridge ions, and the $x^2 - y^2$ ($|x\rangle$) and $3z^2 - r^2$ ($|z\rangle$) orbitals at corner ions (see Fig. 1), with the corresponding electron creation operators: b_i^\dagger , a_{jx}^\dagger , and a_{jz}^\dagger . The hopping elements are: $t_1(\phi) = t \sin \phi$, $t_2(\phi) = t \cos \phi$, and $\phi = \frac{\pi}{6}$, with t standing for the hopping between two identical directional orbitals along the bond $\langle ij \rangle$, i.e., $3x^2 - r^2$ orbitals along the bond $\langle ij \rangle \parallel a$ axis. The phase factors $(-1)^{\lambda_{ij}}$ follow from the alternating orbital phases due to the zig-zag pattern, with $\lambda_{ij} = 1$ or $\lambda_{ij} = 0$, where the hopping connects from the bridge position B_1 or B_2 with the corner site C , respectively.

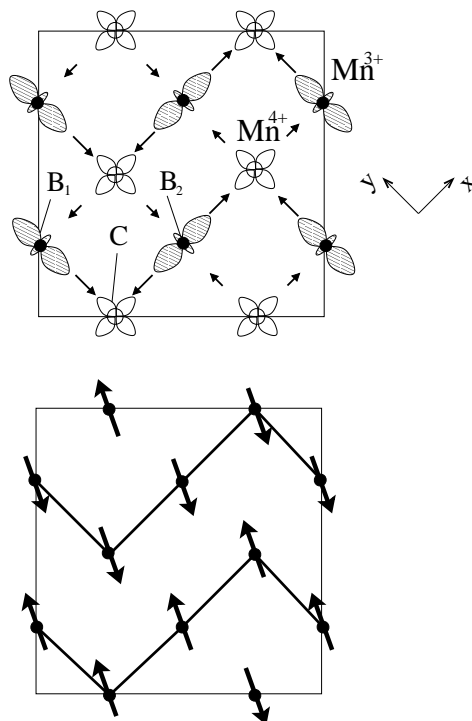


FIG. 1. Schematic picture of the charge and orbital (top panel), and of the spin configuration (bottom panel) for the CE phase. The arrows in the upper panel indicate the in-plane oxygen distortions around the manganese site at the bridge (B_1, B_2) and corner (C) position, which induce the coupling between the e_g electrons and the JT distortions $\{q_i\}$, as discussed in the text. The length of the arrows in the top panel is related to the amplitude of the distortion as due to the JT polaronic term.

The JT orbital polarization interaction (4) splits off two e_g orbitals at site i , if a neighboring site $j(i)$ is occupied by a hole. This interaction has a similar form to that deduced for orbital polarons²⁶ — it favors the occupancy of the directional $|\zeta\rangle$ orbital, oriented along the bond $\langle ij \rangle$, over the orthogonal to it planar $|\xi\rangle$ orbital (e.g., $|3x^2 - r^2\rangle$).

over $|y^2 - z^2\rangle$ orbital for a bond along a axis). The classical (phonon) variable q_i stands for the respective oxygen distortions around an electron at site i , either a bridge or a corner position along the chain (Fig. 1), while g is the coupling constant between e_g electrons and distortions of MnO_6 octahedra, and k_{JT} is the spring constant for the JT mode distortions. It is convenient to introduce the JT energy, defined by $E_{JT} = g^2/k_{JT}$, which is naturally given by the scaling of $q_i = (g/k_{JT})\tilde{q}_i$, where g/k_{JT} is the typical length scale for the JT distortion. By means of these substitutions, H_{JT} reads as:

$$H_{JT} = E_{JT} \sum_i \left[\sum_{j(i)} \tilde{q}_i (n_{i\zeta} - n_{i\xi})(1 - n_j) + \frac{1}{2} \tilde{q}_i^2 \right]. \quad (5)$$

The JT term couples corner and bridge sites in an (a, b) plane, either along the considered zigzag chain, or between two adjacent chains. We minimized the total energy $\langle \mathcal{H}_{\text{pol}} \rangle$ to eliminate the phonon variables $\{\tilde{q}_i\}$, which gives the electronic Hamiltonian solved selfconsistently with:

$$\tilde{q}_i = - \sum_{j(i)} \langle (n_{i\zeta} - n_{i\xi})(1 - n_j) \rangle. \quad (6)$$

The classical variables at bridge and corner positions are different, as suggested by different oxygen distortions around Mn ions.²⁴ If one considers the form of \tilde{q}_i , it is easy to recognize that the distortions are weak within this approximation, if the populations of the two orbitals are the same. Moreover, even in presence of a homogeneous orbital distribution, a small distortion pattern might be induced by the nearest neighbor orbital correlations.

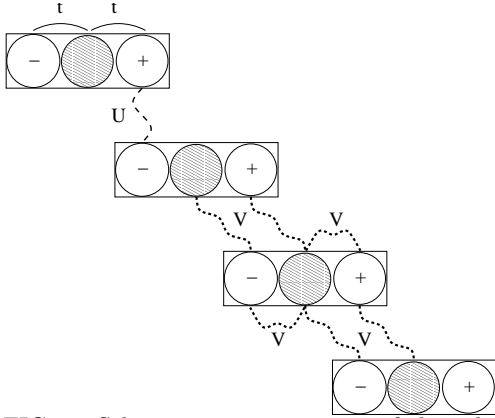


FIG. 2. Schematic representation of the orbital structure in the MM. The chain is divided into molecular triads constituted of a bridge configuration (gray circle) together with an odd (circle with $-$) and even (circle with $+$) superposition of the corner orbitals. The solid line shows the hopping processes inside the molecule, while the dashed lines indicate the intra- and inter-molecular interactions which result from the U and V coupling.

We would like to point out that the form of the interaction between the JT modes and the e_g electrons is

different from that usually assumed, where the on-site Q_2 and Q_3 mode are coupled to the local orbital density.¹⁹ As regards the present model, we are assuming that a directional JT (Q_3 like) mode, with its direction selected by the considered bond $\langle ij \rangle$, is activated by the presence of a hole on the neighbor manganese, thus inducing a non-local correlated dynamics between the lattice and the charge degrees of freedom. As a direct consequence of this non-local coupling, one ends up with an effective directional Coulomb interaction between nearest neighbor manganese which strongly influences both the ground state and the properties of the low-energy excitations.

B. Stability of the CE phase

We begin with the investigation of stability of the CE phase with respect to the C phase, which consists of linear FM chains along the b axis staggered in the a direction, using the mean-field (MF) approximation. The C phase (01) is described by \mathcal{H}_{pol} (1) at $\phi = \frac{\pi}{2}$, with the hopping element t between directional $3y^2 - r^2$ orbitals along each FM chain. While the on-site Coulomb element U increases the energy of the CE phase, it plays no role in the C phase, as the $x^2 - z^2$ orbitals are empty. Thus, the C phase is favored above $U \simeq 2.7t$ ($U \simeq 12.0t$) in the MF (ED) method, if $E_{JT} = 0$. We have verified that increasing E_{JT} induces in MF a charge disproportionation δn in both phases, but this effect is more pronounced in the CE phase, lowering its energy especially when $E_{JT} > t$. Thus, we recognize that the JT term \mathcal{H}_{JT} in Eq. (1) is the main stabilizing mechanism of the observed CE phase.²⁷ The JT term induces a charge ordering (coexisting with orbital ordering), which is in principle unlimited and may come close to $\delta n = 1$, unlike the weak charge ordering induced by the Coulomb interaction U , for which the order parameter cannot exceed $\delta n = 0.19$.¹⁴ Already at $U = 0$ the charge order is more pronounced than that induced by $U \rightarrow \infty$ in a broad range of $E_{JT} > 0.7t$ (Fig. 3). At finite E_{JT} the charge disproportionation is only weakly enhanced by the on-site Coulomb element U . Although the form of the JT interaction term is different, our results agree qualitatively with the recent *ab initio* density-functional calculations.²⁸

TABLE I. Eigenstates and eigenenergies for a molecular unit i in the MM ($\phi = \frac{\pi}{4}$) at $U = E_{JT} = 0$. The bonding, nonbonding, and antibonding states are labelled as $|B\rangle$, $|N\rangle$, and $|A\rangle$.

state	creation operator	energy
$ B\rangle$	$B_i^\dagger = \frac{1}{\sqrt{2}}b_i^\dagger + \frac{1}{2}(a_{i-1,+}^\dagger + a_{i+1,-}^\dagger)$	$E_B = -\sqrt{2}t$
$ N\rangle$	$N_i^\dagger = \frac{1}{\sqrt{2}}(a_{i-1,+}^\dagger - a_{i+1,-}^\dagger)$	$E_N = 0$
$ A\rangle$	$A_i^\dagger = \frac{1}{\sqrt{2}}b_i^\dagger - \frac{1}{2}(a_{i-1,+}^\dagger + a_{i+1,-}^\dagger)$	$E_A = \sqrt{2}t$

The CE phase ground state could also be reproduced by intersite Coulomb interactions in the *electronic* model,¹⁷

$$\mathcal{H}_{\text{elec}} = H_t + H_U + H_V, \quad (7)$$

with $H_V = V \sum_{\langle ij \rangle} n_i n_j$. Taking $V \simeq \frac{1}{2} E_{\text{JT}}$ the models (1) and (7) lead indeed to similar MF phase diagrams. This might suggest that $\mathcal{H}_{\text{elec}}$ could also provide a valid explanation for the observed CE phase. However, going *beyond* the MF one finds that the two models are fundamentally different and lead to qualitatively different results, both for the ground state,²⁹ and for the excitation spectra.

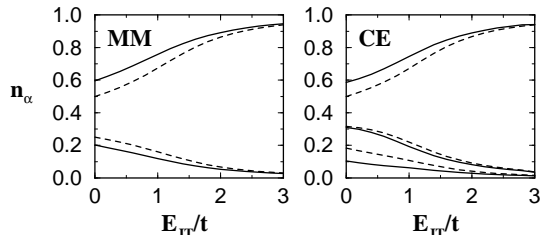


FIG. 3. Electron densities n_α : n_b , n_x and n_z from top to bottom, as functions of E_{JT} , obtained using ED for the chain of $L = 12$ atoms at $U = 0$ (dashed lines) and at $U = 10t$ (solid lines) in: MM ($\phi = \frac{\pi}{4}$), and CE phase ($\phi = \frac{\pi}{6}$).

C. Molecular model

Perhaps the most peculiar feature of the CE phase is the topological frustration of the kinetic energy which occurs due to conflicting orbital phases,¹² and leads to a band insulator already at $U = E_{\text{JT}} = 0$.²⁶ We emphasize that this frustration is maximized when the hopping elements with the opposite phases precisely compensate each other, i.e., $t_1 = t_2 = \frac{1}{2}t$, in the MM at $\phi = \frac{\pi}{4}$ (see Fig. 2). Transforming then the orbital basis $\{a_{ix}^\dagger, a_{iz}^\dagger\}$ to even and odd symmetry states at each corner site:

$$a_{i\pm}^\dagger = \frac{1}{\sqrt{2}}(a_{iz}^\dagger \pm a_{ix}^\dagger), \quad (8)$$

one finds that the hopping term simplifies to:

$$H_t = t \sum_{i=2n} \left(b_i^\dagger a_{i-1,+} + b_i^\dagger a_{i+1,-} + \text{H.c.} \right), \quad (9)$$

and represents a superposition of molecular units. Each of them consists of a central ($i = 2n$) bridge orbital b_i^\dagger , an even symmetry $a_{i-1,+}^\dagger$ orbital at the preceding site $i - 1$, and an odd symmetry $a_{i+1,-}^\dagger$ orbital at the following site $i + 1$, with the eigenstates given in Table I.

In the ground state at half doping,

$$|\Phi_0\rangle = \prod_i B_i^\dagger |0\rangle, \quad (10)$$

all e_g electrons are confined to individual molecular units and occupy the bonding states, and the energy per site $E_{\text{MM}} = -0.707t$ is significantly lower than in the CE phase, $E_{\text{CE}} = -0.695t$. It is interesting to realize that although the electrons are now partly localized within the molecular units, the kinetic energy is at the minimum allowed in the subspace of $t_1^2 + t_2^2 = t^2$.

While the density distribution $\{n_\alpha\}$ ($\alpha = b, x, z$) is uniform for the noninteracting electrons, with the same density at bridge ($n_b = n_x + n_z$) and corner (n_c) positions, increasing U or E_{JT} polarizes the system and induces a charge transfer towards bridge atoms. The effect of U is somewhat more pronounced in the MM than in the CE phase. This is best illustrated by considering the Gutzwiller projected state at $U = \infty$,¹⁴ which leads to the kinetic energy:

$$\tilde{H}_t = t \sum_{i=2n} \left(b_i^\dagger \tilde{a}_{i-1,+} + b_i^\dagger \tilde{a}_{i+1,-} + \text{H.c.} \right), \quad (11)$$

where $\tilde{a}_{j,\pm} = a_{j,\pm}(1 - n_{j,\mp})$ are the electron annihilation operators in the restricted space which does not contain double occupancies. By decoupling the quartic terms in \tilde{H}_t ,¹⁴ $b_i^\dagger a_{j,\pm} n_{j,\mp} \simeq b_i^\dagger a_{j,\pm} \langle n_{j,\mp} \rangle + \langle b_i^\dagger a_{j,\pm} \rangle n_{j,\mp}$, we have found a somewhat larger charge anisotropy $\delta n = n_b - (n_x + n_z) \simeq 0.28$ for the MM than 0.19 found before in the CE phase.¹⁴ A much stronger charge anisotropy, however, is induced in both cases by the JT term; with increasing E_{JT} it approaches gradually the localized limit, and at $E_{\text{JT}} = 2t$ one finds already $\delta n > 0.65$ (Fig. 3), with $n_x > n_z$ due to the different hopping elements in the CE phase. The on-site Coulomb repulsion (3) is invariant under the transformation to $\{|+\rangle, |-\rangle\}$ orbitals and gives the interaction $U n_{i-} n_{j+}$ between two electrons from adjacent molecular units in the MM. It is quite remarkable that the effect of U in the ground state is weak in the regime of $E_{\text{JT}} > t$ (Fig. 3). This demonstrates that the correlation effects are *partly suppressed* by the coupling to the lattice, similar as for the on-site JT term.¹⁹

III. THE OPTICAL CONDUCTIVITY

We now turn to the optical excitations and analyze the evolution of the optical gap Δ with the increasing Coulomb interactions and the JT coupling. The charge gap has been extracted by the calculation of the optical conductivity $\sigma(\omega)$ within a generalization of the Lanczos diagonalization technique.²⁵ Since the system is in an insulating state, one can restrict the calculation of $\sigma(\omega)$ to the finite frequency response given by the Kubo formula

$$\sigma(\omega) = \frac{1 - e^{-\beta\omega}}{\omega} \text{Re} \int_0^\infty d\tau e^{i\omega\tau} \langle j(\tau)j \rangle, \quad (12)$$

where $\beta = 1/k_B T$ and j stands for the contribution of the current operator along the FM zig-zag chain, obtained by the projection at the $x(y)$ direction:

$$j = i \sum_{\langle lm \rangle, \alpha} t_{lm} R_{lm} (b_l^\dagger a_{m\alpha} - a_{m\alpha}^\dagger b_l^\dagger). \quad (13)$$

Here R_{lm} is the component of the vector which connects nearest neighbor sites l and m , t_{lm} is the hopping element between bridge and corner sites as defined above, and $\alpha = (x, z)$, respectively. By applying an electric field along the zig-zag chain, shown in Fig. 1, one accelerates charge along the chain, either along the x or along y axis, depending on the bond direction. In this way the current includes the charge-transfer processes from B_1 or B_2 to C sites, and *vice versa*.

A. Interaction effects in the optical spectra

First, we investigate the charge transport along the chain by analyzing the position of the lowest energy excitation in the optical spectra, which allows to extract the dependence of the optical gap on the value of the JT coupling constant and the electron-electron interaction parameters. Noninteracting electrons give a band structure gap $\Delta_0 = t$ in the CE phase (shown in Fig. 4),²³ and $\Delta_0 = \sqrt{2}t$ in the MM. The on-site repulsion U typically enhances the energy of local excitations in the correlated systems, and increases the optical gap.³⁰ Thus, it was unexpected that the gap first *decreases* linearly with U at $E_{JT} = 0$, and next *saturates* at finite $\Delta \simeq 0.7\Delta_0$ in the regime of $U \gg t$, both in the CE phase and in the MM (Fig. 5). This behavior can be understood, however, by considering the lowest optical excitation in the MM for $U \simeq t$, $|\Phi_i\rangle = N_i^\dagger B_i |\Phi_0\rangle$, and expanding the interaction term $\propto U n_{i-} n_{j+}$ using the Hubbard operators ($X_j^{AB} = A_j^\dagger B_j$, *etcetera*),

$$n_{i\mp 1, \pm} = \frac{1}{4} [X_i^{BB} + X_i^{AA} + 2X_i^{NN} - X_i^{AB} - X_i^{BA} \mp \sqrt{2}(X_i^{AN} + X_i^{NA} - X_i^{BN} - X_i^{NB})]. \quad (14)$$

Indeed, the diagonal term $\propto X_i^{NN}$ enhances the excitation energy by $\frac{1}{8}U$, suggesting that the gap Δ should increase. However, in spite of the electron localization within the molecular units, the above excitation is not localized, but *can propagate* along the chain due to the terms $\propto X_i^{BN} X_{i+2}^{NB}$ in Eq. (14) [see Fig. 6(a)] with dispersion $-\frac{1}{4}U \cos k$, resulting in a *decrease* of the optical gap calculated at band minimum, $\Delta \simeq \Delta_0 - \frac{1}{8}U$.

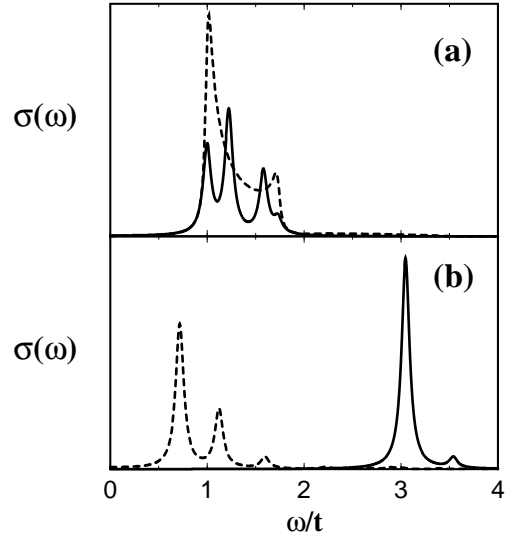


FIG. 4. Optical spectra $\sigma(\omega)$ as obtained in ED for the chain of $L = 12$ atoms in the polaronic model (1) with $\phi = \frac{\pi}{6}$, and for: (a) $U = E_{JT} = 0$, ED result (full line) compared with an exact spectrum for CE phase (dashed line); (b) $U = 10t$, $E_{JT} = 0$ and $E_{JT} = 1.8t$ (dashed and full line).

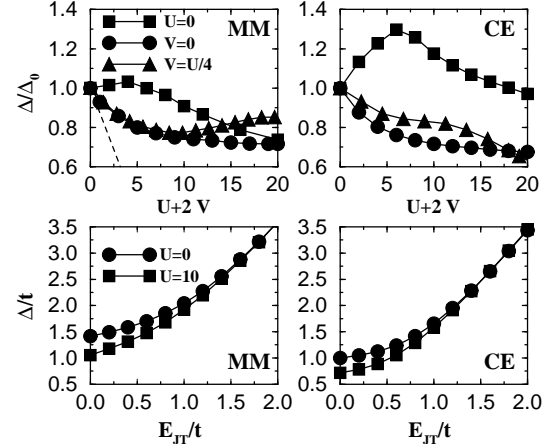


FIG. 5. Optical gaps Δ found in ED for the MM (left) and the CE phase (right) as functions of electron-electron interactions (top): $-U$ (circles), V (squares), and $U + 2V$ for $V = U/4$ (triangles), and of E_{JT} (bottom) for: $U = 0$ (circles) and $U = 10t$ (squares). Dashed line in top left panel shows the weak coupling expansion [Eq. (14)].

A similar weak coupling expansion performed for the intersite Coulomb term $\propto V$ in Eq. (7) gives rise in lowest order to the same optical excited state $\{|\Phi_i\rangle\}$, but it cannot propagate as now $\mathcal{H}_{\text{elec}}$ does not contain terms of the form $\propto X_i^{BN} X_{i+2}^{NB}$. Therefore, acting on such states by $\mathcal{H}_{\text{elec}}$ leads only to higher energy local excitations [Fig. 6(b)], and explains why the optical gap increases first in the range of $2V \lesssim 5t$, before it starts to decrease at higher values of V (Fig. 5). However, in the realistic regime of parameters ($V \ll U$ and $V \propto U$) the gap would decrease, as dominated by the on-site term U . The gaps in the CE

phase follow the same trends when the electron interactions are increased (Fig. 5), with the optical gap being reduced to $\Delta \simeq 0.7t$ at $U = 10t$ (Fig. 4). Thus, the weak propagation along the zigzag chain at $\phi = \frac{\pi}{6}$ does not change the generic picture of the gap decreasing with U , which emerges in the MM.

In contrast, the interactions with the lattice described by the JT term lead to qualitatively different physics. Increasing E_{JT} decreases local potentials at bridge positions in the MM, and thus the splitting between the $|B\rangle$ and $|N\rangle$ state and the gap value Δ *increase*. Although the gaps in the MM and CE phase are different in the realistic regime of $E_{JT} \simeq t$, they approach the same limit $\Delta \simeq 2E_{JT}$ at large $E_{JT} \gg t$. Furthermore, even if the JT term contains an effective long-range Coulomb term mediated by the JT distortions, this contribution does not counterbalance the increase of the charge gap due to the splitting between the bridge and corner states.

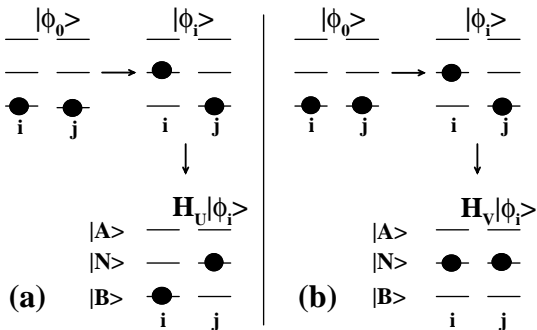


FIG. 6. Schematic representation of the low-energy optical excitations induced in the MM by: (a) on-site U , and (b) intersite V Coulomb interaction. The lowest-energy excitation $|\phi_i\rangle$ is made starting from the ground state $|\phi_0\rangle$. The terms $\propto U$ permute the bonding $|B\rangle$ and non-bonding $|N\rangle$ states on neighboring molecules and allow a propagation of the low-energy excitation along the chain (a), while the terms $\propto V$ provide only the coupling of the low-energy optical excitations to higher energy configurations which contain more than one nonbonding state in the chain (b).

We also investigated the changes in the shape of the optical spectra $\sigma(\omega)$ with increasing interactions. First of all, the asymmetric spectrum for noninteracting electrons, with a large spectral weight at the low-energy feature, is well reproduced (Fig. 4). Both increasing U and E_{JT} lead to more pronounced asymmetry of the spectra. By analyzing the spectral weight distribution, we established that electrons are excited from bridge (Mn^{3+}) to corner (Mn^{4+}) sites, and the x (z) character of the excitations is found predominantly close to the low (high) energy edge. The high energy part loses its spectral weight faster, and the distance between these two features decreases with increasing E_{JT} or U , resulting in much narrower optical spectra [e.g., the distance between two local excitations described by Eq. (11) is only $0.87t$ at $U = \infty$ compared with $1.41t$ at $U = 0$].

B. Finite size scaling

In order to extract information about the electronic system in the thermodynamic limit, we have performed a scaling analysis of the charge gap obtained for different values of the chain lengths (from $L = 4$ to $L = 16$ sites), and two representative sets of parameters with $E_{JT} = 0$: $U = 0, 1, 3$, and $10t$, taking either $V = 0$ or $V = 2t$. We begin with the analysis of the influence of increasing U at $V = 0$ [Fig. 7(a)]. In this case the charge gap is almost independent on the cluster size, which indicates that on-site excitations discussed in the previous Section indeed reduce the optical gap due to correlation effects.

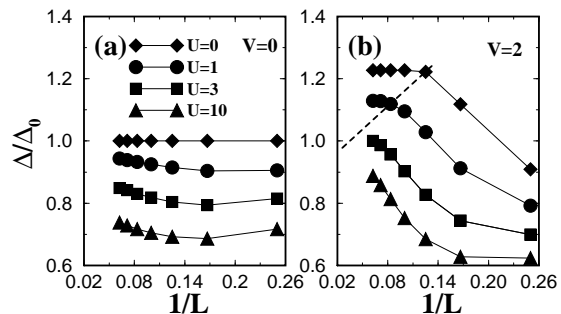


FIG. 7. Optical gap Δ in the CE phase (in the units of the gap for noninteracting electrons Δ_0), found by means of Lanczos diagonalization for different chain size $L = 4, \dots, 16$, for $V = 2t$ and: $U = 0, 1, 3, 10t$. The dashed line in (b) indicates the linear interpolation for the critical size above which the charge gap saturates.

To understand the results at $V = 2t$, let consider first the case of $U = 0$. As shown in the Fig. 7(b), the behavior of the charge gap is monotonic up to $L = 8$ and then it saturates. One can observe that the only effect of V is to confine the charge in the ground state as the lowest charge excitation has a gap in the spectrum, and in addition to localize the lowest optical excitation on a length which is smaller than $L = 8$, as the charge gap does not change above this critical size. In other words, the results suggest that the quantum coherence of the lowest optical excitation extends only over a limited distance, so that when the cluster size exceeds $L = 8$ length, the increasing further cluster size does not affect the value of the charge gap anymore.

Consider now the effect of the on-site interaction $\propto U$. As one can see in the Fig. 7, increasing U reduces the amplitude of the charge gap, and modifies the critical size, above which the gap saturates. Due to the limitation in the numerical computation, we can follow the evolution of the critical size (dashed line) only for $U \simeq t$. Indeed, for large values of $U \gg t$, one observes only a monotonic growth of Δ as a function of $1/L$, without any sign of the gap saturation. We have extracted the behavior of the critical size vs U by means of a linear fit. One can argue

that the effect of U is to increase the localization length in the local optical excitation spectrum (LOES), which yields a larger value of chain size to get a saturation in the charge gap. This itinerant character induced by U is clear in the MM, where we have seen that finite U allows for a propagation of the LOES.

By summarizing the results of the scaling, we deduced that the effect of V is to harden the charge fluctuations in the ground state and to induce a localization of the LOES on a length scale of about $L = 8$. On the contrary, the U term induces an itinerancy in the LOES which manifests itself by an increase of the localization length in the LOES, and consequently of the critical size of saturation of the charge gap. The competition of these two counteracting effects turns out to give the reduction of the charge gap in the bulk limit only for a very weak intersite Coulomb repulsion, $V \ll U$.

A further important conclusion from the presented analysis is that one finds a large range of variation of Δ/Δ_0 , when one moves from a chain of $L = 4$ sites to the extrapolated bulk limit. This analysis might be relevant for real materials if one interprets the disordered high temperature phase of the half-doped manganites as made by a liquid of zig-zag FM chains with different length, so that the optical response has to be built by making a superposition of the response of chains with any size. We argue that the low-energy part of the spectra contains this fluctuating superposition of several chain contributions of different size, and these short-chain contributions are suppressed when one enters into the ordered phase below T_{CO} .

IV. DISCUSSION AND SUMMARY

We argue that the present model agrees qualitatively with available experimental information, and our findings reproduce the experimental observations in $\text{La}_{0.5}\text{Sr}_{1.5}\text{MnO}_4$ ²¹ and $\text{Nd}_{0.5}\text{Ca}_{1.5}\text{MnO}_3$.³¹ In the high temperature regime when the JT distortions are weak, the optical gap is small and dominated by the effect of electronic correlations. When the temperature is decreased below T_{CO} , the spectral weight grows and shifts to higher energy, the optical spectrum is narrowed, and the asymmetry in the spectrum increases. All these features *can be explained* within the present polaronic model (1) as an indication of the onset of the orbital and charge ordering from the disordered state, described by finite values of local variables $\{\tilde{q}_i\}$, and thus increasing orbital polarization due to the JT terms $\propto E_{JT}\tilde{q}_i$. Further shift of the peak feature up to $\Delta \simeq 1.3$ eV would follow from the increased $\{\tilde{q}_i\}$ below the magnetic transition, when the magnetic fluctuations are suppressed. The observed change of the gap Δ is reproduced by $E_{JT} \simeq 1.2t$, which corresponds with $t = 0.4$ eV³ to the expected orbital splitting of ~ 0.3 eV.²⁶

It is worth pointing out that previous studies have

discussed the optical conductivity in the CE phase as due to dipole transitions from $\text{Mn}(e_g)$ to $\text{Mn}(4p)$ states by means of tight-binding approaches and first principle band-structure calculations in the local spin-density approximation.²³ The analysis of Ref. 23 included the effect of the JT distortion as an effective energy level splitting between the bridge and corner states. The proposed interpretation that the changes of the optical spectra are mainly due to the JT distortion on the $\text{Mn}(e_g)$ - $\text{Mn}(4p)$ dipole transitions does not include the effect of correlations, and thus it fails to reproduce the experimentally observed modification of the spectral weight when the temperature is lowered.²¹

Our interpretation of the optical spectra is different. We have shown that the low-energy optical excitations are mainly due to the interband transitions between correlated $\text{Mn}(e_g)$ states. The effect of the JT coupling $\propto E_{JT}$ may be summarized as follows: (i) the uncorrelated spectrum shifts toward higher energy, (ii) the spectral weight increases in the low-energy part, and (iii) the asymmetry of the profile grows as the spectral weight in the high energy shoulder gets suppressed. Particularly the second feature is strongly dependent on the form of the JT coupling. Indeed, by a simple level splitting of the bridge and corner states, one would just obtain a rigid shift of the spectrum, while the effective directional Coulomb interaction present in H_{JT} (5) is responsible of the increase of spectral weight in the low energy side.

Finally, our results show that the shift of the main peak and the increase of its spectral weight come essentially as a consequence of the orbital polarization present in the JT coupling term. It influences the optical transitions between correlated e_g states. The pseudogap activation in the high temperature phase is mainly due to the effect of Coulomb correlation which reduces the band gap. Moreover, as mentioned above, the low energy tail in the spectra observed in the high temperature regime, might originate from the superposition of the optical response of FM zig-zag chains with different length (see Fig. 7).

In summary, we have shown that the subtle interplay between the topology, the Coulomb correlations and the orbital polarization JT terms are responsible for the temperature dependent optical properties of $\text{La}_{0.5}\text{Sr}_{1.5}\text{MnO}_4$. Thus, we argue that these interactions play a crucial role for the observed coexisting orbital and charge ordering in half-doped manganites, which cannot be explained within purely electronic models. When the orbital polarization interaction is taken into account, the charge disproportionation turns out to be much stronger than that induced by U alone, but not as pronounced as in the original Goodenough picture.

ACKNOWLEDGMENTS

We thank P. Horsch and Y. Tokura for valuable discussions. This work was supported by the Committee of

-
- ¹ Y. Tokura and N. Nagaosa, *Science* **288**, 462 (2000).
² A. P. Ramirez, *J. Phys. Cond. Matter* **9**, 8171 (1997).
³ L. F. Feiner and A. M. Oleś, *Phys. Rev. B* **59**, 3295 (1999).
⁴ C. Zener, *Phys. Rev.* **82**, 403 (1951).
⁵ J. B. Goodenough, *Phys. Rev.* **100**, 564 (1955).
⁶ E. O. Wollan and W. C. Koehler, *Phys. Rev.* **100**, 545 (1955).
⁷ A. M. Oleś and L. F. Feiner, *Phys. Rev. B* **65**, 052414 (2002).
⁸ B. J. Sterlieb, J. P. Hill, U. C. Wildgruber G. M. Luke, B. Nachumi, Y. Moritomo, and Y. Tokura, *Phys. Rev. Lett.* **76**, 2169 (1996).
⁹ Y. Tomioka, A. Asamitsu, Y. Moritomo, H. Kuwahara, and Y. Tokura, *Phys. Rev. Lett.* **74**, 5108 (1995); H. Kawano, R. Kajimoto, H. Yoshizawa, Y. Tomioka, H. Kuwahara, and Y. Tokura, *ibid.* **78**, 4253 (1997).
¹⁰ Y. Murakami, H. Kawada, H. Kawata, M. Tanaka, T. Arima, Y. Moritomo, and Y. Tokura, *Phys. Rev. Lett.* **80**, 1932 (1998).
¹¹ K. Nakamura, T. Arima, A. Nakazawa, Y. Wakabayashi, and Y. Murakami, *Phys. Rev. B* **60**, 2425 (1999).
¹² T. Hotta, Y. Takada, H. Koizumi, and E. Dagotto, *Phys. Rev. Lett.* **84**, 2477 (2000).
¹³ I. V. Solovyev and K. Terakura, *Phys. Rev. Lett.* **83**, 2825 (1999).
¹⁴ J. van den Brink, G. Khaliullin, and D. I. Khomskii, *Phys. Rev. Lett.* **83**, 5118 (1999); *ibid.* **86**, 5843 (2001).
¹⁵ S.-Q. Shen, *Phys. Rev. Lett.* **86**, 5842 (2001).
¹⁶ T. Mutou and H. Kontani, *Phys. Rev. Lett.* **83**, 3685 (1999).
¹⁷ G. Jackeli, N. B. Perkins, and N. M. Plakida, *Phys. Rev. B* **62**, 372 (2000).
¹⁸ T. Mizokawa and A. Fujimori, *Phys. Rev. B* **56**, R493 (1997).
¹⁹ S. Yunoki, T. Hotta, and E. Dagotto, *Phys. Rev. Lett.* **84**, 3714 (2000); T. Hotta, A. L. Malvezzi, and E. Dagotto, *Phys. Rev. B* **62**, 9432 (2000).
²⁰ F. Mack and P. Horsch, *Phys. Rev. Lett.* **82**, 3160 (1999).
²¹ T. Ishikawa, K. Ookura, and Y. Tokura, *Phys. Rev. B* **59**, 8367 (1999).
²² J. H. Jung, J. S. Ahn, J. Yu, T. W. Noh, J. Lee, Y. Moritomo, I. Solovyev, and K. Terakura, *Phys. Rev. B* **61**, 6902 (2000).
²³ I. V. Solovyev, *Phys. Rev. B* **63**, 174406 (2001).
²⁴ P. Mahadevan, K. Terakura, and D. D. Sarma, *Phys. Rev. Lett.* **87**, 066404 (2001).
²⁵ J. Jaklič and P. Prelovšek, *Adv. Phys.* **49**, 1 (2000).
²⁶ R. Kilian and G. Khaliullin, *Phys. Rev. B* **60**, 13458 (1999).
²⁷ The CE phase is further stabilized by the AF superexchange terms. While the t_{2g} superexchange is exactly the same in both phases, the stability of the CE phase is further improved by the e_g superexchange in the realistic regime of $U \simeq 10t$.^{3,7} These terms distinguish between different orientation of the occupied e_g orbitals at Mn^{3+} ions and favor the CE phase.
²⁸ Z. Popović and S. Sapaty, *Phys. Rev. Lett.* **88**, 197201 (2002).
²⁹ Taking $U = 10t$ which corresponds to the high-spin charge excitation (Ref. 3), one finds that the CE phase has still a higher energy than the C phase at $V < U/2$ using \mathcal{H}_{elec} . In contrast, the local distortions $\{q_i\}$ which simulate the oxygen distortions are much weaker in the C phase than in the CE phase when \mathcal{H}_{pol} is used, and thus the CE phase is then more stable for the same value of $U = 10t$.
³⁰ H. Eskes, A. M. Oleś, M. Meinders, and W. Stephan, *Phys. Rev. B* **50**, 17980 (1994).
³¹ Y. Okimoto *et al.* unpublished (2002).